IEICE Communications Express, Vol.13, No.3, 60–63

ComEX

LETTER

Effectiveness evaluation of MIMO in polarized OAM multiplexing

Mikito Ito[1], **Shuhei Saito**[1], **Hirofumi Suganuma**[1], **Kayo Ogawa**[2], **and Fumiaki Maehara**[1, a)]

Abstract Adopting polarization for orbital angular momentum (OAM) multiplexing can suppress beam divergence because of using the lower OAM modes, which leads to extending the link distance. In this study, we investigate the effectiveness of multiple-input multiple-output (MIMO) on the polarized OAM multiplexing under the restriction of the same total transmit power and total number of antenna elements. To evaluate the combined effects of polarization and MIMO on system capacity, we conducted computer simulations. Moreover, we investigate the system capacity when only lower OAM modes are available, and compare it with the case without mode limitations. The results of our study provide valuable insights into the potential benefits of using polarization and MIMO for OAM multiplexing.

Keywords: orbital angular momentum (OAM), uniform circular array (UCA), mode multiplexing, polarization, multiple-input multiple-output (MIMO), system capacity

Classification: Wireless communication technologies

1. Introduction

Mobile connectivity is expected to reach more than 70% of the global population by 2023 [1]. Fifth-generation (5G) mobile systems are designed to exceed the capacity of fourth-generation (4G) systems to accommodate future services, including the Internet of Things (IoT) and intelligent transportation systems (ITS) [2]. Moreover, sixth-generation (6G) mobile communication systems, which are to be realized by 2030, will have peak data rates of up to 1 Tb/s, 100-times that of 5G networks, and are expected to provide large-dimensional and autonomous networks that integrate space, air, terrestrial, and underwater networks [3]. Hence, small-cell backhaul and access link technologies must be upgraded to develop advanced mobile systems that support gigabit and terabit connections [4]. In particular, for small-cell backhauls, line-of-sight (LoS) wireless communication with fixed transmitter and receiver locations is more attractive than fiber solutions in terms of flexibility, scalability, and capital expenditure [4]. In this context, orbital angular momentum (OAM) multiplexing has gained increasing attention owing to its potential to simultaneously transmit multiple data streams through a single aperture pair [5, 6, 7, 8, 9].

In OAM multiplexing, the phase front twists along the propagation direction, resulting in a ring-shaped intensity profile. To date, several approaches, such as holographic [5] and spiral phase plates [5, 6] have been proposed to generate OAM signals. However, these approaches require antennas and beam splitters at different locations for mode multiplexing. In contrast, a uniform circular array (UCA) antenna can be considered as a practical approach because using this antenna, the simultaneous transmission of multiple modes can be realized at the same location without beam splitters [7, 8, 9].

Additionally, OAM signals can leverage polarization multiplexing and mode multiplexing to further augment system capacity [10, 11, 12]. Several notable studies have analytically [10, 11] and experimentally [12] examined polarized OAM multiplexing. However, as a distinct multiplexing method from polarization multiplexing, the application of multiple-input multiple-output (MIMO) has proven effective in multiplexing streams within each mode by employing multiple UCAs. Its effectiveness has been evaluated in both experimental [13] and analytical [14] studies. Consequently, it is crucial to elucidate the effects of implementing MIMO and polarization multiplexing under identical hardware conditions.

Hence, this study investigates the efficacy of MIMO in polarized OAM multiplexing while adhering to the constraints of the same total transmit power and total number of antenna elements. Notably, since polarization and MIMO reduce the number of available OAM modes [11], we evaluate the combined effects of polarization and MIMO on system capacity through computer simulations. Furthermore, we assess the impact of mode limitations on system capacity from a practical perspective.

2. Adoption of MIMO for polarized OAM multiplexing

The antenna configuration used in this study is illustrated in Fig. 1. As shown in Fig. 1, the total number of antenna elements was set to $2N_AN$, where N_A and N represent the numbers of UCAs and antenna elements in a UCA, respectively. This configuration allows for a total of $2N_AN$ streams, irrespective of whether polarization or MIMO is used. When polarization is applied, the number of antenna elements assigned to each polarization plane is halved, resulting in a decrease in received power. However, both the vertical and horizontal planes can utilize lower modes that exhibit strong robustness against beam divergence, thus mitigating the power loss. Furthermore, in the case of MIMO with N_A streams and polarization, the number of antenna elements assigned in UCAs is divided by N_A, which can

[1] Graduate School of Fundamental Science and Engineering, Waseda University, 3-4-1 Ohkubo, Shinjuku-ku, Tokyo 169-8555, Japan
[2] Graduate School of Science, Japan Women's University, 2-8-1 Mejirodai, Bunkyou-ku, Tokyo 112-8681, Japan
[a)] fumiaki_m@waseda.jp

DOI: 10.23919/comex.2023XBL0156
Received November 13, 2023
Accepted December 12, 2023
Publicized January 15, 2024
Copyedited March 1, 2024

This work is licensed under a Creative Commons Attribution Non Commercial, No Derivatives 4.0 License.
Copyright © 2024 The Institute of Electronics, Information and Communication Engineers

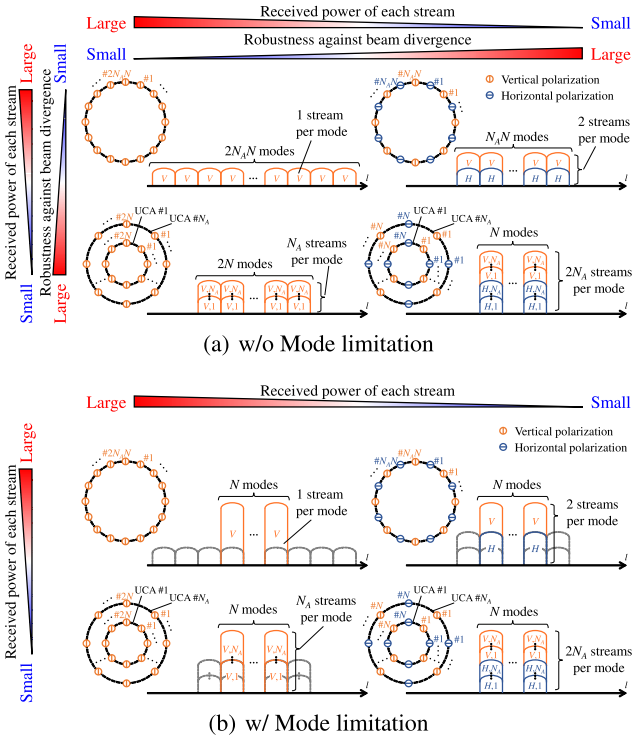

Fig. 1 Antenna configurations for polarized OAM multiplexing with MIMO.

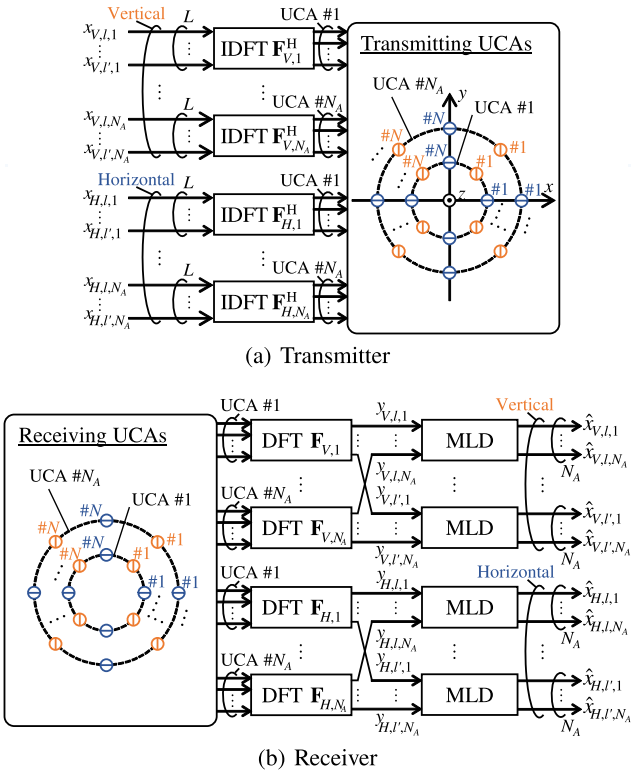

Fig. 2 System configuration of polarized OAM multiplexing with MIMO.

further enhance robustness against beam divergence and degrade the received power of lower modes. However, under realistic conditions where available modes are restricted to lower modes, the number of transmitted streams decreases. In such cases, the power resources allocated to each stream increase, thereby enhancing the system capacity for polarization and MIMO.

We then analyzed the system capacity of polarized OAM-MIMO, as depicted in Fig. 2, where L is the number of multiplexed OAM modes. In our analysis, we assumed maximum likelihood detection (MLD) for MIMO detection, which considers the maximum ratio combining (MRC) gain. Moreover, we considered isotropic antennas as antenna elements and ignored polarization interference. As shown in Fig. 2, the transmit signal vector with polarization $\mathbf{s} \in \mathbb{C}^{2N_A L}$ is expressed as

$$\mathbf{s} = \mathbf{F}^{\mathrm{H}}\mathbf{x}, \tag{1}$$

where $\mathbf{x} \in \mathbb{C}^{2N_A L}$ is the modulated signal vector. $\mathbf{F}^{\mathrm{H}} \in \mathbb{C}^{2N_A N \times 2N_A L}$ is the inverse discrete Fourier transform (IDFT) matrix, which can be expressed as

$$\mathbf{F}^{\mathrm{H}} = \mathrm{diag}\{\mathbf{F}_V^{\mathrm{H}}, \mathbf{F}_H^{\mathrm{H}}\}, \tag{2}$$

$$\mathbf{F}_V^{\mathrm{H}} = \mathrm{diag}\{\mathbf{F}_{V,1}^{\mathrm{H}}, \cdots, \mathbf{F}_{V,N_A}^{\mathrm{H}}\}, \tag{3}$$

$$\mathbf{F}_H^{\mathrm{H}} = \mathrm{diag}\{\mathbf{F}_{H,1}^{\mathrm{H}}, \cdots, \mathbf{F}_{H,N_A}^{\mathrm{H}}\}, \tag{4}$$

where $\mathbf{F}_{V,i}^{\mathrm{H}}$ and $\mathbf{F}_{H,i}^{\mathrm{H}} \in \mathbb{C}^{N \times L}$ $(i = 1, \cdots, N_A)$ are the IDFT matrices of the transmitting UCA #i considering the direction of polarization, where "V" and "H" represent the vertical and horizontal polarization, respectively. In Eqs. (3) and (4), the IDFT component of the m-th antenna element at the l-th mode in each polarization is given by

$$f_{m,l}^{*} = \frac{1}{\sqrt{N}} \exp\left(j\frac{2\pi l m}{N}\right). \tag{5}$$

At the receiver, the received signal vector $\mathbf{y} \in \mathbb{C}^{2N_A L}$ is represented by

$$\mathbf{y} = \mathbf{F}(\mathbf{H}\mathbf{s} + \mathbf{n}) = \mathbf{F}\mathbf{H}\mathbf{F}^{\mathrm{H}}\mathbf{x} + \tilde{\mathbf{n}}, \tag{6}$$

where $\mathbf{n} \in \mathbb{C}^{2N_A N}$ and $\tilde{\mathbf{n}} \in \mathbb{C}^{2N_A L}$ are the noise vectors, and their elements follow the same distribution. $\mathbf{F} \in \mathbb{C}^{2N_A L \times 2N_A N}$ is the discrete Fourier transform (DFT) matrix, which can be expressed as

$$\mathbf{F} = \mathrm{diag}\{\mathbf{F}_V, \mathbf{F}_H\}, \tag{7}$$

$$\mathbf{F}_V = \mathrm{diag}\{\mathbf{F}_{V,1}, \cdots, \mathbf{F}_{V,N_A}\}, \tag{8}$$

$$\mathbf{F}_H = \mathrm{diag}\{\mathbf{F}_{H,1}, \cdots, \mathbf{F}_{H,N_A}\}, \tag{9}$$

where $\mathbf{F}_{V,j}$ and $\mathbf{F}_{H,j} \in \mathbb{C}^{L \times N}$ $(j = 1, \cdots, N_A)$ are the DFT matrices of the receiving UCA #j considering the direction of polarization, respectively. $\mathbf{H} \in \mathbb{C}^{2N_A N \times 2N_A N}$ is the channel matrix, which can be represented by

$$\mathbf{H} = \begin{bmatrix} \mathbf{H}_{V,V} & \mathbf{H}_{V,H} \\ \mathbf{H}_{H,V} & \mathbf{H}_{H,H} \end{bmatrix}, \tag{10}$$

$$\mathbf{H}_{Q,P} = [\mathbf{H}_{Q,P,j,i}]_{Q,P \in \{V,H\}, i,j \in \{1,\cdots,N_A\}}, \tag{11}$$

where $\mathbf{H}_{Q,P,j,i} \in \mathbb{C}^{N \times N}$ is the channel matrix between transmitting UCA #i and receiving UCA #j considering the direction of the polarization, respectively. Assuming free-space propagation, the channel condition between the m-th antenna element in the transmitting UCA #i and the n-th antenna element in the receiving UCA #j is expressed by

$$h_{j,i,n,m} = \frac{\lambda}{4\pi d_{j,i,n,m}} \exp\left(-j\frac{2\pi d_{j,i,n,m}}{\lambda}\right).$$

$$\mathbf{P}(\theta'_{j,i,n,m}, \phi'_{j,i,n,m})^{\mathrm{T}} \cdot \mathbf{P}(\theta_{j,i,n,m}, \phi_{j,i,n,m}), \quad (12)$$

where λ is wavelength and $d_{j,i,n,m}$ is distance between the transmitting and receiving antenna elements, respectively. Moreover, $\theta_{j,i,n,m}$, $\theta'_{j,i,n,m}$ and $\phi_{j,i,n,m}$, $\phi'_{j,i,n,m}$ are the elevation and the azimuth angles, and $\mathbf{P}(\theta_{j,i,n,m}, \phi_{j,i,n,m})$ and $\mathbf{P}(\theta'_{j,i,n,m}, \phi'_{j,i,n,m})$ are the radiation pattern vectors of the transmitting and receiving antenna elements, respectively. Assuming the isotropic antenna as an antenna element, the radiation pattern vectors of these antennas are given by [10]

$$\mathbf{P}(\theta, \phi) = \begin{cases} [1,0]^{\mathrm{T}} & (V\text{-polarization}) \\ [0,1]^{\mathrm{T}} & (H\text{-polarization}) \end{cases}. \quad (13)$$

It should be noted that the radiation pattern in Eq. (13) indicates that the orthogonality among different polarization planes is perfectly retained.

From Eq. (6), the received signal of the l-th OAM mode at the UCA #j in each polarization plane is given by

$$y_{V,l,j} = \left(\sum_{i=1}^{N_A} \sigma_{V,l,j,i} x_{V,l,i} \right) + \tilde{n}_{V,l,j}, \quad (14)$$

$$y_{H,l,j} = \left(\sum_{i=1}^{N_A} \sigma_{H,l,j,i} x_{H,l,i} \right) + \tilde{n}_{H,l,j}, \quad (15)$$

where $x_{V,l,i}$, $x_{H,l,i}$ and $\tilde{n}_{V,l,j}$, $\tilde{n}_{H,l,j}$ are the modulated signal and noise, respectively. Moreover, $\sigma_{V,l,j,i}$ and $\sigma_{H,l,j,i}$ are (l,l) elements of $\mathbf{F}_{V,j}\mathbf{H}_{V,V,j,i}\mathbf{F}^{\mathrm{H}}_{V,i}$ and $\mathbf{F}_{H,j}\mathbf{H}_{H,H,j,i}\mathbf{F}^{\mathrm{H}}_{H,i}$, respectively. From Eqs. (14) and (15), the signal-to-noise ratio (SNR) of the i-th stream in the l-th OAM mode with vertical and horizontal polarization can be expressed as

$$\gamma_{V,l,i} = \sum_{j=1}^{N_A} \frac{|\sigma_{V,l,j,i}|^2 P_{V,l,i}}{P_n}, \quad (16)$$

$$\gamma_{H,l,i} = \sum_{j=1}^{N_A} \frac{|\sigma_{H,l,j,i}|^2 P_{H,l,i}}{P_n}, \quad (17)$$

where $P_{V,l,i} = E[|x_{V,l,i}|^2]$, $P_{H,l,i} = E[|x_{H,l,i}|^2]$ and $P_n = E[|\tilde{n}_{V,l,i}|^2] = E[|\tilde{n}_{H,l,i}|^2]$ are the transmit power and noise power, respectively. Consequently, the system capacity of OAM-MIMO with polarization multiplexing can be calculated as

$$C_{sum} = \sum_{l} \sum_{i=i}^{N_A} \left(\log_2(1 + \gamma_{V,l,i}) + \log_2(1 + \gamma_{H,l,i}) \right). \quad (18)$$

However, the system capacity of OAM-MIMO without polarization multiplexing can be calculated in a similar manner to the polarized case by allocating all the antenna elements to either vertical or horizontal polarization. Therefore, the system capacity of the OAM-MIMO without polarization multiplexing can be calculated as

$$C_{sum} = \begin{cases} \sum_{l} \sum_{i=1}^{N_A} \log_2 \left(1 + \gamma_{V,l,i}\right) & (V\text{-polarization}) \\ \sum_{l} \sum_{i=1}^{N_A} \log_2 \left(1 + \gamma_{H,l,i}\right) & (H\text{-polarization}) \end{cases}. \quad (19)$$

3. Numerical results

The system parameters used in this study are presented in Table I. The total number of antenna elements in the UCAs was set 64, and N_A determines the number of antenna elements in each UCA; N_A was set to 1, 2, or 4, meaning each OAM mode has 1, 2, or 4 stream(s) in each polarization plane, respectively, where the transmit power is the same among all streams; $N_A = 1$ indicates the OAM multiplexing without MIMO. In the ideal case without mode limitation, the number of multiplexed modes L was set to N (OAM

Table I System parameters

Carrier frequency f_c	39 GHz
Total number of antenna elements	64
Radiation pattern	Isotropic
Radii of UCAs	0.60 m ($N_A = 1$)
(Number of UCAs N_A)	0.24, 0.60 m ($N_A = 2$)
	0.24, 0.36, 0.48, 0.60 m ($N_A = 4$)
Total transmit power	23 dBm
Noise power	−80 dBm

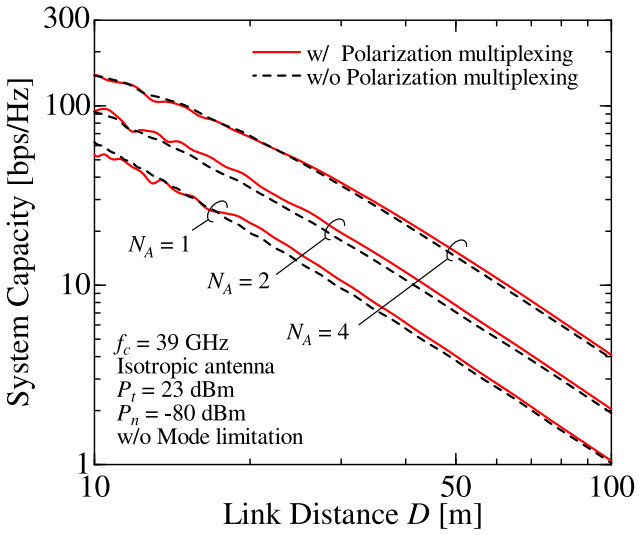

(a) w/o Mode limitation

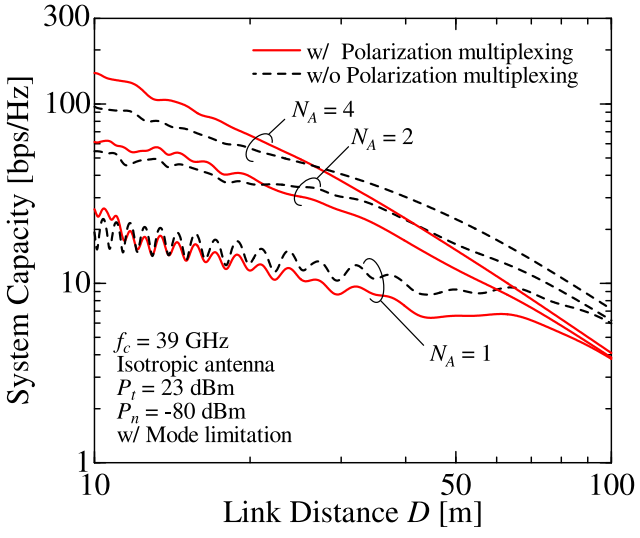

(b) w/ Mode limitation

Fig. 3 System capacity versus link distance D.

modes $l = -N/2+1, \cdots, N/2$) with polarization multiplexing, or $2N$ ($l = -N+1, \cdots, N$) without it, respectively. However, in a realistic case with mode limitation, L was set to 8 ($l = -3, \cdots, 4$) regardless of polarization and MIMO.

Fig. 3 illustrates the system capacity plotted against the link distance, D. First, as shown in Fig. 3(a), in the absence of mode limitations, increasing the number of UCAs N_A can obtain the space diversity benefit obtained from MLD, which improves the system capacity. Moreover, at short link distances, where the influence of beam divergence is small, the system capacity without polarization multiplexing is better than that with polarization multiplexing. This is because the case without polarization multiplexing can use all modes and many receiving elements. On the other hand, for long link distances, the polarization multiplexing case outperforms the case without multiplexing regardless of the number of UCAs because only low OAM modes can be utilized. Next, as shown in Fig. 3(b), it can be seen that, in the presence of mode limitations, the system capacity improves with an increase in the number of UCAs N_A at short link distances with high SNR. On the other hand, over long link distances, the SNR decreases due to propagation attenuation, and the effect of stream power reduction due to the use of MIMO becomes severe, which degrades the effectiveness of MIMO. In particular, at short distances with high SNR, polarization multiplexing can improve system capacity. However, with the increase in the link distance, since the effect of stream power reduction due to the use of polarization multiplexing becomes severe, the system capacity of polarization multiplexing gets worse than the case without polarization multiplexing.

4. Conclusion

This study aimed to examine the effectiveness of MIMO for polarized OAM multiplexing while considering the constraints of the same total transmit power and total number of antenna elements. Considering that the number of MIMO streams and polarization have a direct impact on the available modes and stream power, the combined effects of polarization and MIMO on system capacity were evaluated by computer simulations. Numerical results showed the effectiveness of applying MIMO to polarized OAM multiplexing, regardless of the presence or absence of mode limitations. It was found that by increasing the number of UCAs, the space diversity benefit of MLD can be enhanced, and hence, the system capacity can be improved. Moreover, it was observed that when there are no mode limitations, it is beneficial to apply polarization multiplexing, which can actively utilize lower OAM modes, regardless of the number of UCAs. On the other hand, in practical situations with mode limitations, the application of polarization multiplexing is effective over short link distances with high SNR, but over long link distances with low SNR, polarization multiplexing is not necessarily effective because the influence of stream power reduction becomes severe in the limited number of OAM modes. Therefore, in realistic scenarios with mode limitations, it is crucial to adopt polarization multiplexing and MIMO appropriately, depending on the link distance.

Acknowledgments

This work was supported by JSPS Grant-in-Aid for Scientific Research Grant Number JP22K04112.

References

[1] "Cisco annual internet report (2018–2023)," Cisco, White Paper, March 2020.
[2] M. Shafi, A.F. Molisch, P.J. Smith, T. Haustein, P. Zhu, P.D. Silva, F. Tufvesson, A. Benjebbour, and G. Wunder, "5G: A tutorial overview of standards, trials, challenges, deployment, and practice," *IEEE J. Sel. Areas Commun.*, vol. 35, no. 6, pp. 1201–1221, June 2017. DOI: 10.1109/jsac.2017.2692307
[3] Z. Zhang, Y. Xiao, Z. Ma, M. Xiao, Z. Ding, X. Lei, G.K. Karagiannidis, and P. Fan, "6G wireless networks: Vision, requirements, architecture, and key technologies," *IEEE Veh. Technol. Mag.*, vol. 14, no. 3, pp. 28–41, Sept. 2019. DOI: 10.1109/mvt.2019.2921208
[4] Z. Pi, J. Choi, and R. Heath, "Millimeter-wave gigabit broadband evolution toward 5G: Fixed access and backhaul," *IEEE Commun. Mag.*, vol. 54, no. 4, pp. 138–144, April 2016. DOI: 10.1109/mcom.2016.7452278
[5] F.E. Mahmouli and S.D. Walker, "4-Gbps uncompressed video transmission over a 60-GHz orbital angular momentum wireless channel," *IEEE Wireless Commun. Lett.*, vol. 2, no. 2, pp. 223–226, April 2013. DOI: 10.1109/wcl.2013.012513.120686
[6] Y. Yan, G. Xie, M.P.J. Lavery, H. Huang, N. Ahmed, C. Bao, Y. Ren, Y. Cao, L. Li, Z. Zhao, A.F. Molisch, M. Tur, M.J. Padgett, and A.E. Willner, "High-capacity millimetre-wave communications with orbital angular momentum multiplexing," *Nature Commun.*, vol. 5, no. 4876, pp. 1–9, Sept. 2014. DOI: 10.1038/ncomms5876
[7] S.M. Mohammadi, L.K.S. Daldorff, J.E.S. Bergman, R.L. Karlsson, B. Thidé, K. Forozesh, T.D. Carozzi, and B. Isham, "Orbital angular momentum in radio—A system study," *IEEE Trans. Antennas Propag.*, vol. 58, no. 2, pp. 565–572, Feb. 2010. DOI: 10.1109/tap.2009.2037701
[8] D. Lee, H. Sasaki, H. Fukumoto, K. Hiraga, and T. Nakagawa, "Orbital angular momentum (OAM) multiplexing: An enabler of a new era of wireless communications," *IEICE Trans. Commun.*, vol. E100-B, no. 7, pp. 1044–1063, July 2017. DOI: 10.1587/transcom.2016sci0001
[9] R. Chen, M. Zou, X. Wang, and A. Tennant, "Generation and beam steering of arbitrary-order OAM with time-modulated circular arrays," *IEEE Syst. J.*, vol. 15, no. 4, pp. 5313–5320, Dec. 2021. DOI: 10.1109/jsyst.2020.3019337
[10] L. Sung, D. Park, and D.-H. Cho, "Performance analysis of orbital angular momentum (OAM) transmission using dual polarization antenna based uniform circular array architecture," Proc. 2016 13th IEEE Annu. Consum. Commun. Netw. Conf. (CCNC 2016), pp. 517–522, Jan. 2016. DOI: 10.1109/ccnc.2016.7444834
[11] Y. Ito, S. Saito, H. Suganuma, K. Ogawa, and F. Maehara, "Effectiveness evaluation of polarization in OAM multiplexing," *IEICE Commun. Express*, vol. 10, no. 4, pp. 199–205, April 2021. DOI: 10.1587/comex.2020xbl0184
[12] M. Hirabe, Z. Ryuji, H. Miyamoto, K. Ikuta, and E. Sasaki, "40 m transmission of OAM mode and polarization multiplexing in E-band," Proc. 2019 IEEE Globecom Workshops (GC Wkshps 2019), pp. 1–6, Dec. 2019. DOI: 10.1109/gcwkshps45667.2019.9024495
[13] D. Lee, H. Sasaki, H. Fukumoto, Y. Yagi, T. Kaho, H. Shiba, and T. Shimizu, "An experimental demonstration of 28 GHz band wireless OAM-MIMO (orbital angular momentum multi-input and multi-output) multiplexing," Proc. 2018 IEEE Veh. Technol. Conf. (VTC 2018-Spring), pp. 1–5, June 2018. DOI: 10.1109/vtcspring.2018.8417790
[14] S. Saito, H. Suganuma, K. Ogawa, and F. Maehara, "Performance enhancement of OAM-MIMO using successive interference cancellation," Proc. 2019 IEEE Veh. Technol. Conf. (VTC 2019-Spring), pp. 1–5, April 2019. DOI: 10.1109/vtcspring.2019.8746501